catalysts

MDPI

Article

Thermal Stability and Potential Cycling Durability of Nitrogen-Doped Graphene Modified by Metal-Organic Framework for Oxygen Reduction Reactions

Harsimranjit Singh, Shiqiang Zhuang, Bharath Babu Nunna and Eon Soo Lee *

Advanced Energy Systems and Microdevices Laboratory, Department of Mechanical and Industrial Engineering, New Jersey Institute of Technology, Newark, NJ 07102, USA; hs523@njit.edu (H.S.); sz86@njit.edu (S.Z.); bn63@njit.edu (B.B.N.)

* Correspondence: eonsoo.lee@njit.edu; Tel.:973-596-3318

Received: 30 October 2018; Accepted: 27 November 2018; Published: 3 December 2018

Abstract: Here we report a nitrogen-doped graphene modified metal-organic framework (N-G/MOF) catalyst, a promising metal-free electrocatalyst exhibiting the potential to replace the noble metal catalyst from the electrochemical systems; such as fuel cells and metal-air batteries. The catalyst was synthesized with a planetary ball milling method, in which the precursors nitrogen-functionalized graphene (N-G) and ZIF-8 are ground at an optimized grinding speed and time. The N-G/MOF catalyst not only inherited large surface area from the ZIF-8 structure, but also had chemical interactions, resulting in an improved Oxygen Reduction Reaction (ORR) electrocatalyst. Thermogravimetric Analysis (TGA) curves revealed that the N-G/MOF catalyst still had some unreacted ZIF-8 particles, and the high catalytic activity of N-G particles decreased the decomposition temperature of ZIF-8 in the N-G/MOF catalyst. Also, we present the durability study of the N-G/MOF catalyst under a saturated nitrogen and oxygen environment in alkaline medium. Remarkably, the catalyst showed no change in the performance after 2000 cycles in the N_2 environment, exhibiting strong resistance to the corrosion. In the O_2 saturated electrolyte, the performance loss at lower overpotentials was as low compared to higher overpotentials. It is expected that the catalyst degradation mechanism during the potential cycling is due to the oxidative attack of the ORR intermediates.

Keywords: oxygen reduction reaction; metal-organic framework; nitrogen-doped graphene; rotating disk electrode; durability study; potential cycling

1. Introduction

The sluggish Oxygen Reduction Reaction (ORR) kinetics is the major barrier in renewable-energy technologies such as fuel cells and metal-air batteries [1]. Therefore, over the past few decades, research on sustainable energy conversion and storage systems has focused primarily on improving reaction kinetics through the synthesis of advanced materials. However, when it comes to commercial applications, Platinum Group Metal (PGM) catalyst materials still dominate these systems [2]. Due to the excessive cost and limited reserves of PGM catalysts, it is imperative to replace these materials with inexpensive, high performance, and durable non-PGM catalysts [2,3].

To replace PGM catalysts, non-PGM catalysts should have; (i) volumetric activity larger than 1/10 that of Pt/C, (ii) specific surface area larger than 200 m^2/g, and (iii) high stability and durability under the operating conditions. Nowadays, nitrogen-doped graphene (N-G) catalysts are emerging as promising catalysts for the ORR. It is known that the doping of nitrogen onto

graphene induces uneven charge distribution of carbon atoms, which improves oxygen adsorption and reduction [4]. Nevertheless, these N-G catalysts exhibit insufficient activity due to their poor electronic conductivity and poor stability resulting from the corrosion of active sites during ORR [4]. Therefore, various nitrogen-containing precursors and templates have been used to synthesize N-G catalysts, in order to achieve the above requirements [4–6]. These advances include the use of metal-organic frameworks (MOF) as an addition to N-G catalysts for augmenting the porosity and specific surface area of the catalysts structure, to enhance the mass transport properties of ORR relevant species. MOF's are composite materials built from metal ions coordinated with organic ligands to form one-, two-, or three-dimensional structures. Specifically, the zeolite imidazolate frameworks (ZIF) formed by multimember rings of ZnN_4 and CoN_4, in which zinc or cobalt atoms are linked with nitrogen atoms by imidazolate links that are widely used to synthesize porous carbon supports. These carbon-based nanomaterials synthesized by utilizing ZIFs not only have a controlled porosity, but also tend to have an easy functionalization with other heteroatoms.

In the past decade, significant advances have been made in the non-PGM catalyst technology, which caused it to become commercially viable [4,5,7,8]. Despite these improvements in electrocatalytic activities, very little attention has been provided to the stability and durability of non-PGM catalysts, which is the remaining obstacle in the commercialization process. In general, the catalyst degradation mechanism of non-PGM catalysts includes; (i) leeching of the metal active site [9–11]; (ii) oxidative attack of the ORR intermediates such as H_2O_2, and HO_2^- [12]; (iii) protonation of the active site [13]; and (iv) carbon support corrosion during the potential cycling [14,15]. In the case of the metal-based electrocatalysts such as Fe or Co, leeching of active sites is the most observed degradation mechanism, which led most researchers to either eliminate metal-based catalysts or develop new synthetic synthesis approaches to surround the metal active sites by a protective graphite layer [16,17]. On the other hand, the absence of metal active sites in metal-free catalysts makes them more suitable candidates for the ORR.

In general, ORR catalysts are synthesized by conventional methods like chemical vapor deposition (CVD), thermal treatment, and plasma treatment [18]. In most of these methods, the activation energy for synthesis reactions is derived from heat energy; however, the resultant catalysts have insufficient nitrogen doping and poor electronic conductivity despite exhibiting a porous structure [19]. Caking issues, overheating, and safety hazards are some of the other issues associated with these methods. Therefore, in this research we have adopted a mechanochemical approach called ball milling to synthesize the nitrogen-doped graphene modified with metal-organic framework (N-G/MOF). Specifically, the nanoscale high energy wet (NHEW) ball milling method was implemented, in which the activation energy was obtained from collisions of the grinding balls and the precursor materials. Various parameters such as the grinding speed and grinding time were carefully controlled to optimize the catalyst's ORR catalytic activity [20–22]. The electrochemical performance (current density) of N-G/MOF catalysts was better than the 10 wt % Pt/C catalyst under similar experimental conditions [22].

The primary objectives of this research include: (1) The durability study (performance lost following potential cycling) of metal-free N-G/MOF catalysts in both O_2 and N_2 saturated electrolyte; and (2) understand the effect of N-G particles on MOF particles during the synthesis process. The study was conducted with characterizing techniques such as electron microscopy for the morphological study, Brunauer–Emmett–Teller (BET) for understanding the effect of MOF on the specific surface area, Thermogravimetric Analysis (TGA) for investigating the thermal effect of N-G particles on the MOF particles during the synthesis process, Rotating Disk Electrode (RDE) technique for the potential cycling, and chronoamperometric response of the catalyst in methanol.

2. Results and Discussion

The synthesis mechanism of the N-G and N-G/MOF catalysts is shown in Figure 1. In this study, we developed an inexpensive and scalable method for preparing the N-G/MOF catalyst. In the

NHEW ball milling synthesis method the grinding speed and time were the main parameters that controlled the final morphology, chemical structure, and the electrochemical performance of the catalyst. Therefore, after several iterations, the optimum performance of the N-G catalyst was found after 16 h at 500 RPM [20,21]. It was found that, on increasing the grinding time, the particle size decreased and nitrogen-doping content kept on increasing, but the most advantageous grinding time for the highest current density and electron transfer number was 16 h. The N-G catalyst exhibited almost similar performance as the 10 wt % Pt/C catalyst, however, it was concluded that there was room for improvement [20]. This improvement was made possible with the integration of state-of-the-art metal-organic framework materials in the N-G catalyst. The precursor material was ground for 16 h, and the grinding speed was controlled and varied, because the high energy from the ball mill can impact the physical and chemical properties of the ZIF-8 particles. It was observed that at 350 RPM the catalyst showed the optimum current density, which was even higher than current density of 10 wt % Pt/C [22]. This increase in the electrochemical performance of the catalyst was attributed to the micro porosity induced by the ZIF-8 structure and the chemical interactions of N-G and ZIF-8 particles, which increased the pyridinic active sites on the imidazolate framework and also enhanced the surface density of the active sites for improved ORR [22–24].

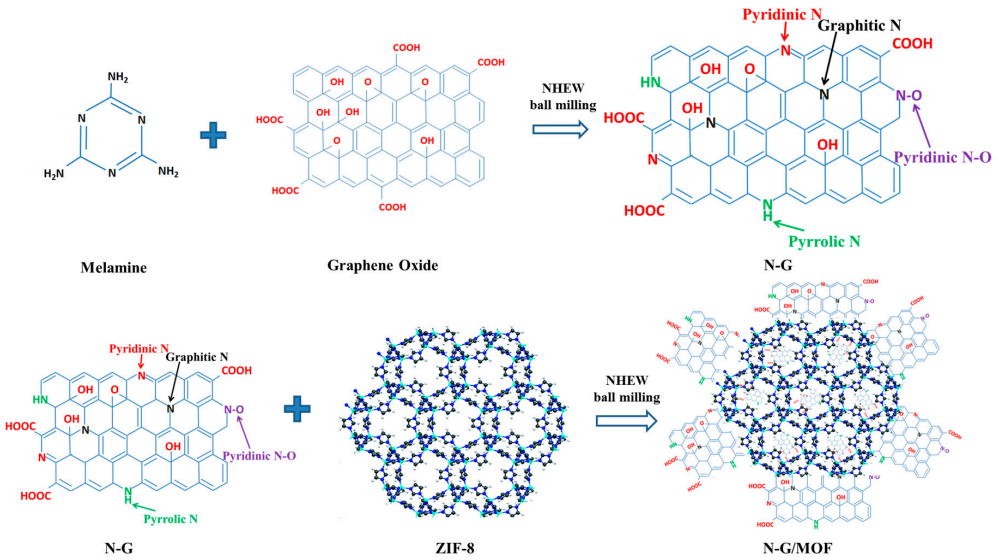

Figure 1. Synthesis of N-G/MOF catalyst from ZIF-8 and N-G precursors by the Nanoscale High Energy Wet (NHEW) ball milling method.

2.1. Morphology

The catalytic performance of the ORR catalyst depends on both the physical (particle size, surface structure, and porosity) and chemical (nitrogen doping, active site density, and surface density) characteristics of the material. Therefore, in this study the catalysts surface structure and particle size were studied with Scanning Electron Microscopy (SEM), Transmission Electron Microscopy (TEM), and Zetasizer Nano ZS techniques. Figure 2a,b shows the flaky structure of the N-G catalyst. The NHEW ball milling synthesis method cleaved and crushed the long sheets of the graphene oxide (GO) creating defects for unhindered nitrogen doping, resulting in an amorphous structure with a reduced surface area. The particle size distribution of the N-G-16-500, ZIF-8, N-G/MOF-350 are shown in Figure 3. The particle size of the N-G-16-500 catalyst was reduced from the micrometer scale of GO down to the range of 150–1700 nm averaging around 459 nm. Figure 2c,d shows the crystalline rhombic dodecahedral structure of the ZIF-8 with a particle size of 3090 nm. It can be seen from Figure 2e,f that the N-G/MOF catalyst had both amorphous and crystalline structures inherited from N-G and MOF structures, with an average particle size of 955 nm. From our previous study, it was

proven that nitrogen-doping and particle size can be controlled by the grinding speed and grinding time of ball milling [20–22].

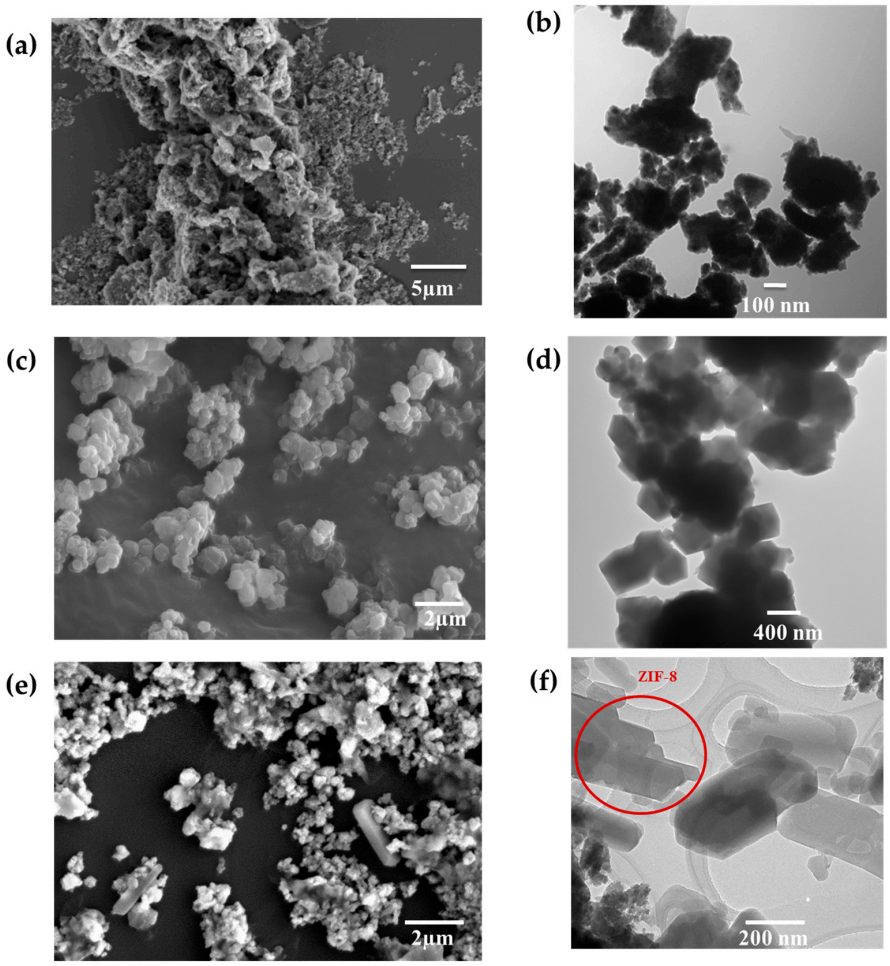

Figure 2. Scanning Electron Microscope (SEM) and Transmission Electron Microscope (TEM) Images of (**a**,**b**) N-G, (**c**,**d**) ZIF-8, and (**e**,**f**) N-G/MOF-350.

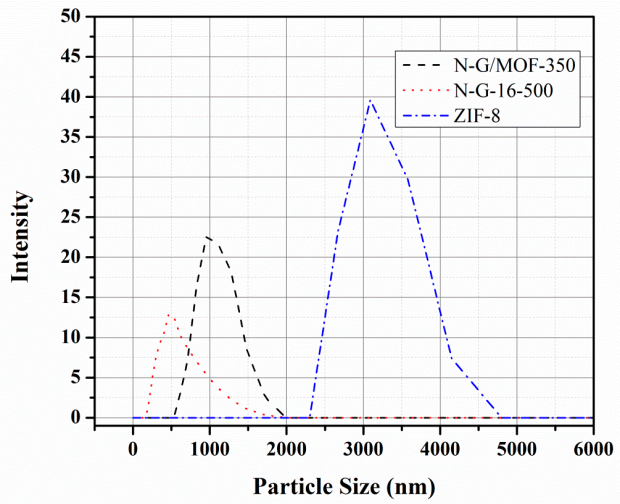

Figure 3. Particle size of N-G-16-500, ZIF-8, and N-G/MOF-350.

2.2. BET Surface Area

The surface area, pore volume, and pore size of GO, N-G, N-G/MOF-350, and ZIF-8 were analyzed through the Brunauer–Emmett–Teller (BET) Autosorb instrument (Quantachrome) with N_2 as an adsorbate. It can be observed from Table 1, after the NHEW ball milling of GO and melamine precursors, the BET surface area of N-G catalyst was reduced to 77.81 m^2/g in contrast to the 347.23 m^2/g of GO. During the synthesis process, the GO sheets were cleaved and crushed by the grinding conditions, which resulted in the decrease in the BET surface area, porosity, and average pore size. The surface area of as-received ZIF-8 was also analyzed to investigate the effect of ZIF-8 particles on the structure of the final N-G/MOF-350 catalyst. It was expected that the BET surface area of the final N-G/MOF-350 (1039.79 m^2/g) catalyst would be lower than the as-received ZIF-8 (1775.4 m^2/g), because of the NHEW ball milling. This decrease in the surface area was because of the change in the crystalline morphology of ZIF-8 to a mixture of amorphous and crystalline of N-G/MOF-350. This morphological change resulted in the loss of the free volume of the porous ZIF-8 structure and dispersion of the N-G particles over the ZIF-8 particles, which block the internal microporous structure. However, the N-G/MOF-350 catalyst still has significantly large surface area and enhanced electronic conductivity required for commercial applications.

Table 1. Physical characteristics of GO, N-G, ZIF-8, and N-G/MOF [23].

Characteristics/Materials	Graphene Oxide	N-G-16-500	ZIF-8	N-G/MOF-350
BET Surface Area (m^2/g)	347.23	77.81	1775.4	1039.79
Pore Volume (cc/g)	0.4	0.08	0.62	0.42
Avg. Pore Size (nm)	2.76	1.4	1.1	1.08

2.3. Thermogravimetric Analysis

The TGA curves in the nitrogen atmosphere are presented in Figure 4. The thermal stability of the N-G, N-G/MOF, ZIF-8, and a control group using ground ZIF were analyzed using the Perkin Elmer 1 Thermo Gravimetric Analyzer (20 °C/min). To investigate the behavior of ZIF-8 in the synthesis of N-G/MOF catalyst, a control group of ZIF-8 was ground in DI water (wet environment) at 350 RPM. The initial 15% weight loss in the Ground ZIF was attributed to the desorption of the water molecules. The decomposition temperature for ZIF-8 is 375 °C, which was quite similar to the decomposition temperature of the ground ZIF-8. This observation confirmed that 350 RPM energy of the ball milling in the wet environment does not impact the thermal properties of the ZIF-8. Till 330 °C, the decomposition of N-G and N-G/MOF had a similar trend. After 330 °C, 7% weight loss was observed in the N-G/MOF catalyst due to the decomposition of the MOF structure. It was confirmed that the N-G/MOF structure still had some unreacted MOF particles which was also observed in the TEM image (Figure 2f), and the addition of N-G catalyst to the MOF particles lowered the decomposition temperature of the unreacted MOF in the N-G/MOF catalyst.

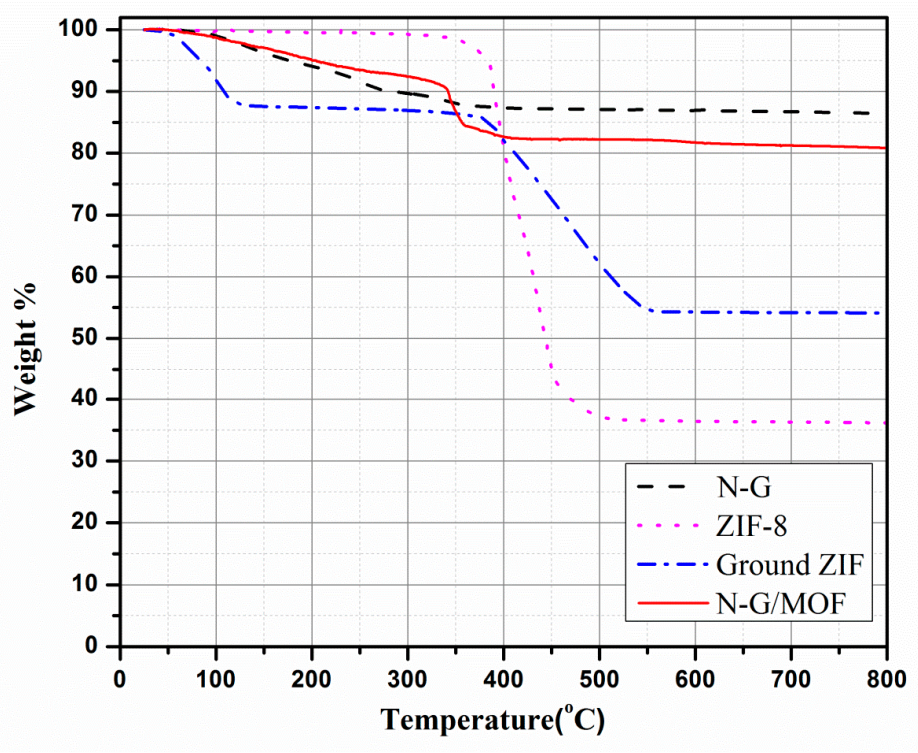

Figure 4. TGA curves of N-G-16-500, ZIF-8, N-G/MOF-350, and control group grounded ZIF.

2.4. Durability Study of N-G/MOF and N-G

The durability test for the ORR of the catalyst was performed by cycling the potential from 0.3 V to 1.1 V vs. Reference Hydrogen Electrode (RHE) for 2000 cycles (CV) at 150 mV/s scan rate in a continuous flow of nitrogen and oxygen saturated environment. The chronoamperometric response of the N-G/MOF catalyst was also collected at a constant voltage of −0.43 V for 4000 s with 10% (v/v) methanol at 1600 RPM. As discussed earlier, the degradation mechanism of ORR catalysts resulted from the corrosion of the carbon support, or due to the deactivation of the active sites during ORR. Therefore, to correctly investigate the degradation mechanism of the N-G/MOF catalyst, the electrolyte was saturated with nitrogen and oxygen respectively.

The durability of the catalyst support can be studied by cycling the potential in the absence of ORR species, such as in a nitrogen-saturated environment. Theoretically, the corrosion of the carbon support is thermodynamically possible above 0.207 V versus Standard Hydrogen Electrode (SHE) [25]. Figure 5a shows the cyclic voltammetry (CV) curve of the N-G and N-G/MOF catalyst before and after 2000 cycles. In the case of N-G catalyst, the CV curve of the catalyst remained similar even after 2000 cycles, suggesting the high durability of the GO as catalyst support. In the case of N-G/MOF catalysts, in which the MOF decomposed due to the catalytic action of N-G to create more pyridinic active sites and also acted as support for the catalyst, the CV profile was unchanged even after 2000 cycles. This observation clearly indicated that even though the morphology of the N-G/MOF catalyst was a mixture of amorphous and crystalline nature, there was no degradation of the graphene oxide and MOF support. To the contrary, it is well known that the graphitic carbon supports are more corrosion-resistant compared to amorphous supports. It is also argued that in the absence of platinum as catalyst, the potential range for investigating the oxidation of the carbon support should be above 1.0 V vs. RHE [9]. This argument is valid because in the case of fuel cells, which are exposed to start-up and shutdown cycles, the cathode potential can go higher than 1.2 V. Therefore, separate potential cycling experiments were conducted in which the catalyst was degraded between the potential ranges of 1.1 V to 1.4 V vs. RHE. To compare the performance, the CV tests were carried out before and after 2000 cycles in the higher oxidation potential range. It can be observed from Figure 5b that there was

no change in reduction potential or the onset potential of the N-G/MOF catalyst even after cycling the potential in the higher oxidation range. Therefore, it should be acknowledged that the N-G/MOF catalyst exhibited remarkable resistance to the corrosion of the support in the N_2 environment.

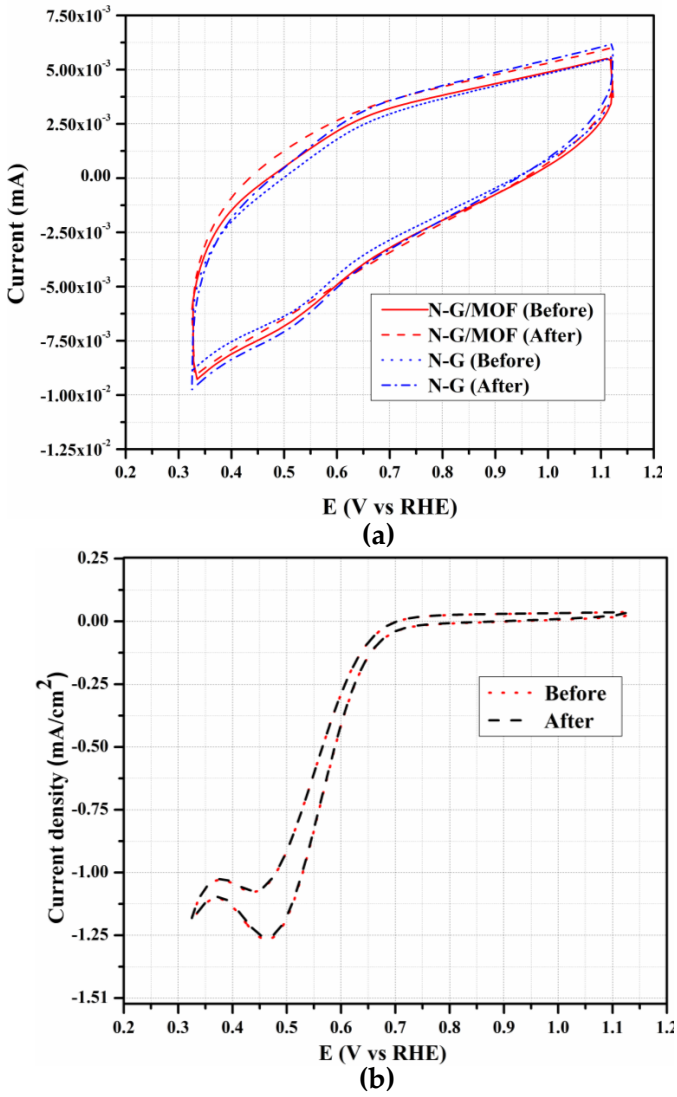

Figure 5. (**a**) Potential cycling durability study of N-G and N-G/MOF catalysts in nitrogen saturated conditions, and (**b**) cyclic voltammogram (O_2 saturated 0.1 M KOH) of N-G/MOF catalyst before and after higher oxidation potentials.

To investigate the degradation/deactivation of N-G and N-G/MOF catalysts, the catalysts were subjected to potential cycling experiments in the O_2-saturated electrolyte. Since there is no oxidation/corrosion of carbon support in the nitrogen-saturated electrolyte, any loss of performance in the oxygen-saturated electrolyte would be attributed to the ORR intermediates, which can either deactivate the active sites or aid in the degradation of carbon support. Figure 6a shows the degradation of N-G and N-G/MOF catalysts in the presence of O_2. After 2000 cycles, the N-G/MOF catalyst retained 58.2% of its initial performance (peak current density), in contrast to 38.1% of N-G catalyst. It can also be observed from Figure 6a,b that in the case of the N-G catalyst, the reduction peak almost vanished and the durability performance of the N-G catalyst was much closer to the as-received GO than the N-G/MOF catalyst. Moreover, the N-G/MOF catalyst retained its reduction peak indicating higher potential cycling durability than the N-G catalyst. It was evident from the above observations that the integration of MOF particles in the N-G catalyst not only enhanced the electrochemical performance

(current density), but also increased the durability in the O_2-saturated electrolyte. Furthermore, we investigated the performance loss of the N-G/MOF catalyst at different overpotentials (Figure 6c). In the lower overpotential region, the catalyst lost 19.9% and 17% of its initial performance at 0.7 V and 0.65 V respectively, whereas at higher overpotential regions such as 0.5 V and 0.47 V the catalyst lost 40.47% and 41.8%. The performance loss due to the potential cycling was significantly large at higher overpotentials compared to lower overpotentials. It has been reported that in the metal catalysts, the performance loss is dominant in the initial cycles followed by a more gradual decrease [16]. This initial performance loss was predominantly because of the leeching of the metal active sites from the surface of the catalyst or the protonation of the metal active site in the acidic environment [13]. The absence of metal active site in the N-G/MOF catalyst resulted in a gradual decrease in the performance of the catalyst rather than a sudden drop as in the case of metal catalysts during the durability study. The formation H_2O_2 in acidic medium, or HO_2^- in alkaline medium and other ORR intermediates are known to be the main contributors for the degradation of ORR catalysts. It has been reported by Ramaswamy et al. that ORR intermediates act as electron withdrawing-groups depleting the carbon surface of the π-electrons [25]. Additionally, it is known that H_2O_2 is an oxidizing agent; it can attack the nitrogen functional groups, which are the active sites for metal-free ORR catalysts. Therefore, it is expected that the catalyst degradation mechanism of the metal-free N-G/MOF catalyst is the oxidative attack of these intermediates on the carbon support and the active sites.

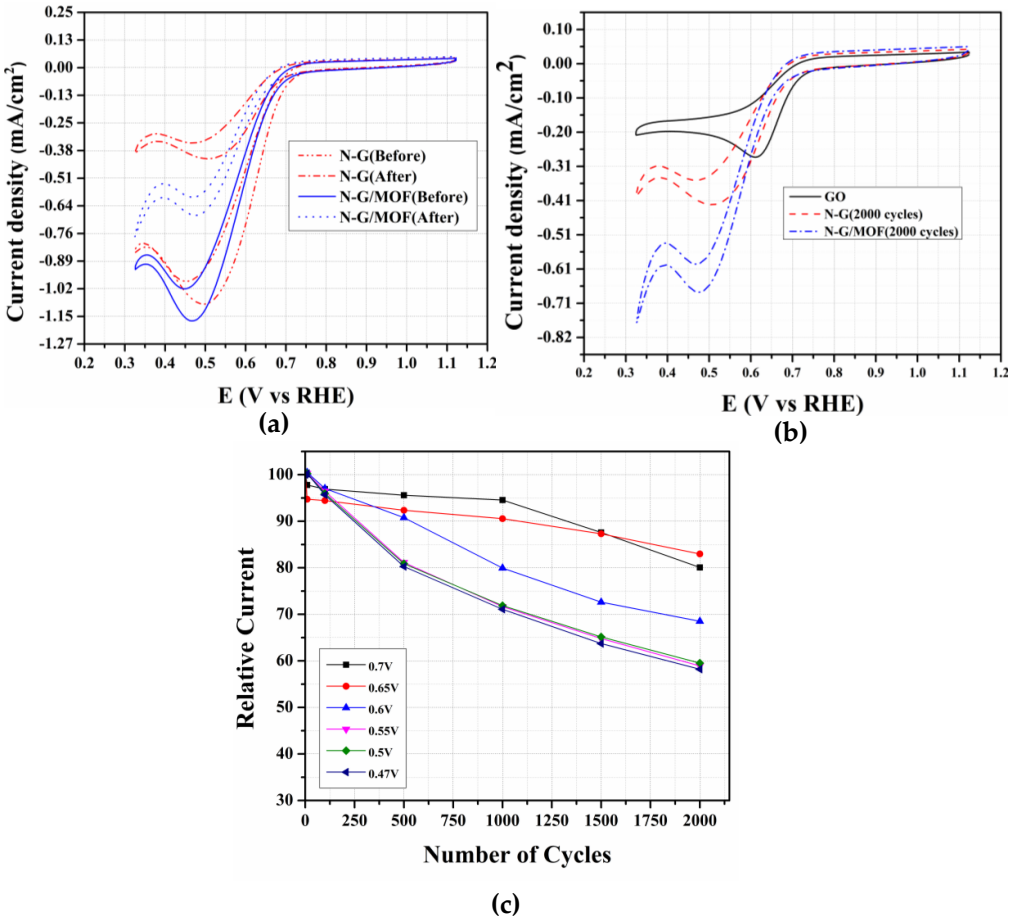

Figure 6. (**a**) Cyclic voltammetry of N-G and N-G/MOF catalyst in oxygen-saturated 0.1 M KOH solution before and after 2000 cycles, (**b**) the performance of N-G and N-G/MOF catalyst after potential cycling compared with the graphene oxide and, and (**c**) N-G/MOF-350 catalyst Rotating Disk Electrode (RDE) performance at various potentials after cycling the potential between 0.3 V to 1.1 V vs. Reference Hydrogen Electrode (RHE).

2.5. Effect of Methanol Crossover

To assess the selectivity of the N-G/MOF as an ORR catalyst, the methanol crossover effect was investigated. Particularly, in Direct Methanol Fuel Cell (DMFC), crossover of methanol from anode to cathode can result in the poisoning of the catalyst and ultimately loss in the equilibrium electrode potential. Therefore, a good electrocatalyst should be inert to the methanol oxidation. Figure 7 shows the effect of methanol oxidation on N-G/MOF and 10 wt % Pt/C catalysts. As shown, the Pt/C showed a strong response to the methanol oxidation, resulting in more than 50% loss in the performance spontaneously. However, no obvious response was observed in the N-G/MOF catalyst under the same testing conditions. Therefore, it can be concluded that the N-G/MOF catalyst exhibits high selectivity and strong tolerance against methanol oxidation.

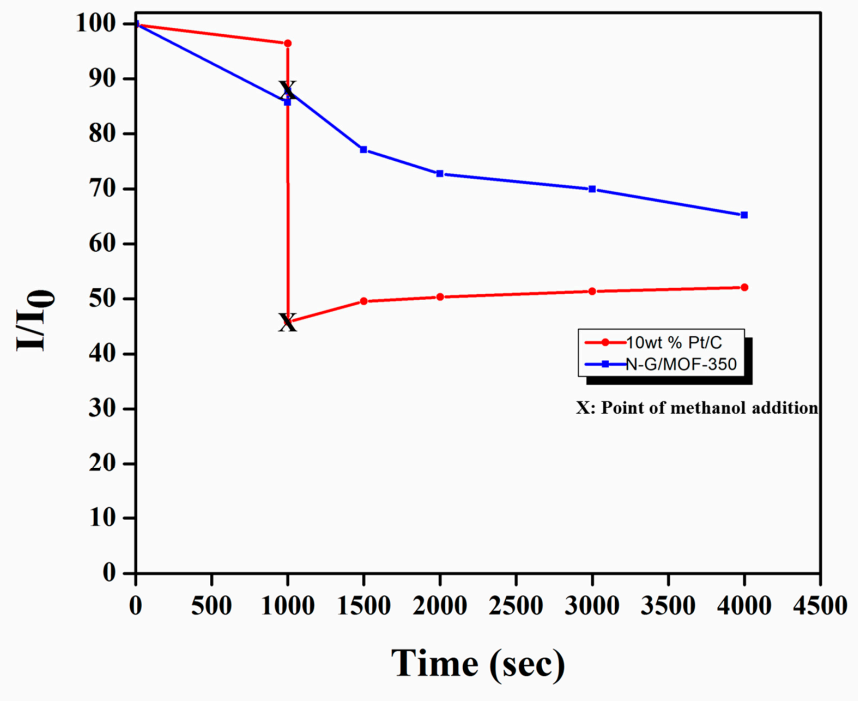

Figure 7. Chronoamperometric responses of N-G/MOF and 10 wt % Pt/C catalysts in oxygen-saturated 0.1 M KOH at 0.47 V and 1600 RPM in 10% v/v methanol.

3. Experimental Methods

3.1. Materials

Graphene oxide (5 mg/mL, H.C, Graphene Supermarket, GO), melamine (99%, Aldrich, St. Louis, MO, USA, $C_3H_6N_6$), ZIF-8 ((Basolite Z1200, formula $C_8H_{10}N_4Zn$, Aldrich, powder, produced by BASF), potassium hydroxide (0.1 M, Aldrich, KOH), methanol (99%, Aldrich, CH_3OH), and Nafion solution (5 wt %, Aldrich) were used for the material synthesis and characterizations.

3.2. Synthesis

N-G catalyst was synthesized in the high energy ball milling machine (Retsch PM-100, North Rhine-Westphalia, Germany) with graphene oxide (GO) and melamine (nitrogen source) as the precursors. To avoid the container contamination and unnecessary large aggregates of GO, the precursors were mixed in 8 mL of deionized water. The N-G catalyst precursor solution (GO:Melamine 1:6) was ultrasonicated for 20 min and heated at 60 °C to dissolve all the melamine in the solution. The solution was then transferred to a 12 mL stainless steel jar containing zirconia grinding balls (diameter 1.4–1.7 mm) and grinded for 16 h at 500 RPM. The final N-G/MOF catalyst

material was prepared by taking the N-G catalyst solution and ZIF-8 (1:1) as the precursor materials and grinding for 16 h at 350 RPM. The synthesized catalyst solution was then centrifuged in the 0.1 M NaOH solution and deionized water to remove the dissoluble components. The filtered solution was the dried to obtain the N-G/MOF-350 catalyst particles.

3.3. Catalyst Ink Preparation

1 mg of the catalyst (N-G and N-G/MOF) and 4 µL of 0.5 wt % Nafion solution were dispersed in 1 mL of DI water and ultrasonicated for 20 min. Fifteen µL of the catalyst ink was pipetted on the working electrode and then dried at 60 C to create a loading of 76.43 $\mu g/cm^2$.

3.4. Electrochemical Characterizations

All of the durability studies of the N-G, N-G/MOF and Pt/C catalysts were characterized with Rotating Disk Electrode method using RRDE-3A (ALS Co., Ltd., Tokyo, Japan) and CH Instruments work station. The measurements were carried out in the 0.1 M KOH electrolyte solution at room temperature with glassy carbon as working electrode (0.19625 cm^2), platinum coil as counter electrode and 0.1 M KOH-Hg/HgO as the reference electrode. Prior to the characterizations, the working electrode was polished with 1µm polishing diamond and then with 0.05 µm polishing alumina to obtain mirror-like surface and then rinsed with DI water and ethanol. Before the measurements the electrolyte solution was purged with nitrogen gas for 20 mins and scanned several times until the curve was stabilized. All the potentials were converted to RHE by the following general relation:

$$E_{RHE} = E_{Hg/HgO} + 0.059\ pH + E^0{}_{Hg/HgO}$$

where, $E^0{}_{Hg/HgO} = 0.098$ V, and $E_{Hg/HgO}$ is the measured potential [26].

4. Conclusions

In summary, we have synthesized metal-free nitrogen-doped graphene modified with metal organic framework catalyst by a mechanochemical approach. This novel catalyst improved specific surface area and enhanced surface active site density because of the chemical interactions between the N-G and MOF particles. Through TGA curves it was concluded that there was still some unreacted MOF particles in the N-G/MOF catalyst and due to the addition of the N-G catalyst, the decomposition temperature of the ZIF-8 in the N-G/MOF catalyst was decreased from 375 °C to 338 °C, proving the chemical interactions between the N-G and MOF particles. We also conducted durability studies of the N-G/MOF catalyst in the oxygen and nitrogen saturated alkaline solution. The N-G/MOF catalyst had strong resistance towards carbon corrosion in the nitrogen-saturated electrolyte; therefore, the anticipated degradation mechanism of the catalyst was the oxidative attack of intermediates produced during the ORR. The integration of MOF particles in N-G catalyst improved the durability of the catalyst. Moreover, the N-G/MOF catalyst showed superior stability and better selectivity towards methanol crossover as compared to 10 wt % Pt/C catalyst.

Author Contributions: H.S., S.Z. and E.S.L. conceived and designed the experiments; H.S. performed the experiments; H.S. and E.S.L. analyzed the data; H.S. and B.B.N. contributed in material procurement; H.S. and E.S.L. wrote the paper.

Funding: This research received no external funding.

Acknowledgments: The authors acknowledge the research support from the Materials Characterization Laboratory at Otto H. York center (NJIT), Advanced Energy Systems and Microdevices Laboratory (NJIT). This research was carried out in part at the Center for Functional Materials, Brookhaven National Laboratory, which is supported by the US Department of Energy, Office of Basic Energy Sciences, under Contract No. DE-SC0012704. We would also like to thank the administrative support from the department of Mechanical and Industrial Engineering at NJIT.

Conflicts of Interest: The authors declare no conflicts of interest.

References

1. Wei, W.; Tao, Y.; Lv, W.; Su, F.Y.; Ke, L.; Li, J.; Wang, D.W.; Li, B.; Kang, F.; Yang, Q.H. Unusual high oxygen reduction performance in all-carbon electrocatalysts. *Sci. Rep.* **2014**, *4*, 6289. [CrossRef] [PubMed]
2. Gasteiger, H.A.; Kocha, S.S.; Sompalli, B.; Wagner, F.T. Activity benchmarks and requirements for Pt, Pt-alloy, and non-Pt oxygen reduction catalysts for PEMFCs. *Appl. Catal. B Environ.* **2005**, *56*, 9–35. [CrossRef]
3. Serov, A.; Robson, M.H.; Halevi, B.; Artyushkova, K.; Atanassov, P. Highly active and durable templated non-PGM cathode catalysts derived from iron and aminoantipyrine. *Electrochem. Commun.* **2012**, *22*, 53–56. [CrossRef]
4. Zhong, H.X.; Wang, J.; Zhang, Y.W.; Xu, W.L.; Xing, W.; Xu, D.; Zhang, Y.F.; Zhang, X.B. ZIF-8 Derived Graphene-Based Nitrogen-Doped Porous Carbon Sheets as Highly Efficient and Durable Oxygen Reduction Electrocatalysts. *Angew. Chem. Int. Ed.* **2014**, *53*, 14235–14239. [CrossRef] [PubMed]
5. Jahan, M.; Bao, Q.; Loh, K.P. Electrocatalytically active graphene–porphyrin MOF composite for oxygen reduction reaction. *J. Am. Chem. Soc.* **2012**, *134*, 6707–6713. [CrossRef] [PubMed]
6. Lin, Z.; Song, M.K.; Ding, Y.; Liu, Y.; Liu, M.; Wong, C.P. Facile preparation of nitrogen-doped graphene as a metal-free catalyst for oxygen reduction reaction. *Phys. Chem. Chem. Phys.* **2012**, *14*, 3381–3387. [CrossRef] [PubMed]
7. Strickland, K.; Miner, E.; Jia, Q.; Tylus, U.; Ramaswamy, N.; Liang, W.; Sougrati, M.T.; Jaouen, F.; Mukerjee, S. Highly active oxygen reduction non-platinum group metal electrocatalyst without direct metal–nitrogen coordination. *Nat. Commun.* **2015**, *6*, 7343. [CrossRef]
8. Proietti, E.; Jaouen, F.; Lefèvre, M.; Larouche, N.; Tian, J.; Herranz, J.; Dodelet, J.P. Iron-based cathode catalyst with enhanced power density in polymer electrolyte membrane fuel cells. *Nat. Commun.* **2011**, *2*, 416. [CrossRef]
9. Banham, D.; Ye, S.; Pei, K.; Ozaki, J.I.; Kishimoto, T.; Imashiro, Y. A review of the stability and durability of non-precious metal catalysts for the oxygen reduction reaction in proton exchange membrane fuel cells. *J. Power Sources* **2015**, *285*, 334–348. [CrossRef]
10. Wang, B. Recent development of non-platinum catalysts for oxygen reduction reaction. *J. Power Sources* **2005**, *152*, 1–15. [CrossRef]
11. Deng, D.; Yu, L.; Chen, X.; Wang, G.; Jin, L.; Pan, X.; Deng, J.; Sun, G.; Bao, X. Iron encapsulated within pod-like carbon nanotubes for oxygen reduction reaction. *Angew. Chem.* **2013**, *125*, 389–393. [CrossRef]
12. Schulenburg, H.; Stankov, S.; Schünemann, V.; Radnik, J.; Dorbandt, I.; Fiechter, S.; Bogdanoff, P.; Tributsch, H. Catalysts for the oxygen reduction from heat-treated iron (III) tetramethoxyphenylporphyrin chloride: Structure and stability of active sites. *J. Phys. Chem. B* **2003**, *107*, 9034–9041. [CrossRef]
13. Liu, G.; Li, X.; Popov, B. Stability study of nitrogen-modified carbon composite catalysts for oxygen reduction reaction in polymer electrolyte membrane fuel cells. *ECS Trans.* **2009**, *25*, 1251–1259.
14. Wu, G.; More, K.L.; Johnston, C.M.; Zelenay, P. High-performance electrocatalysts for oxygen reduction derived from polyaniline, iron, and cobalt. *Science* **2011**, *332*, 443–447. [CrossRef] [PubMed]
15. Peng, H.; Mo, Z.; Liao, S.; Liang, H.; Yang, L.; Luo, F.; Song, H.; Zhong, Y.; Zhang, B. High performance Fe-and N-doped carbon catalyst with graphene structure for oxygen reduction. *Sci. Rep.* **2013**, *3*, 1765. [CrossRef]
16. Bashyam, R.; Zelenay, P. A class of non-precious metal composite catalysts for fuel cells. *Nature* **2006**, *443*, 63–66. [CrossRef] [PubMed]
17. Manzoli, M.; Boccuzzi, F. Characterisation of Co-based electrocatalytic materials for O_2 reduction in fuel cells. *J. Power Sources* **2005**, *145*, 161–168. [CrossRef]
18. Wang, H.; Maiyalagan, T.; Wang, X. Review on recent progress in nitrogen-doped graphene: Synthesis, characterization, and its potential applications, 10.1021/cs200652. *ACS Catal.* **2012**, *2*, 781–794. [CrossRef]
19. Xu, H.; Ma, L.; Jin, Z. Nitrogen-doped graphene: Synthesis, characterizations and energy applications. *J. Energy Chem.* **2017**, *27*, 146–160. [CrossRef]
20. Zhuang, S.; Lee, E.S.; Lei, L.; Nunna, B.B.; Kuang, L.; Zhang, W. Synthesis of nitrogen-doped graphene catalyst by high energy wet ball milling for electrochemical systems. *Int. J. Energy Res.* **2016**, *40*, 2136–2149. [CrossRef]

21. Zhuang, S.; Nunna, B.B.; Boscoboinik, J.A.; Lee, E.S. Nitrogen-doped graphene catalysts: High energy wet ball milling synthesis and characterizations of functional groups and particle size variation with time and speed. *Int. J. Energy Res.* **2017**, *41*, 2535–2554. [CrossRef]
22. Zhuang, S.; Nunna, B.B.; Lee, E.S. Metal organic framework-modified nitrogen-doped graphene oxygen reduction reaction catalyst synthesized by nanoscale high-energy wet ball-milling structural and electrochemical characterization. *MRS Commun.* **2018**, *8*, 40–48. [CrossRef]
23. Singh, H.; Zhuang, S.; Nunna, B.B.; Lee, E.S. Morphology and Chemical Structure of Modified Nitrogen-Doped Graphene for Highly Active Oxygen Reduction Reactions. In Proceedings of the 48th Power Source Conference, Denver, CO, USA, 14 June 2018.
24. Zhuang, S.; Singh, H.; Nunna, B.B.; Mandal, D.; Boscoboinik, J.A.; Lee, E.S. Nitrogen-doped graphene-based catalyst with metal-reduced organic framework: Chemical analysis and structure control. *Carbon* **2018**, *139*, 933–944. [CrossRef]
25. Ramaswamy, N.; Tylus, U.; Jia, Q.; Mukerjee, S. Activity descriptor identification for oxygen reduction on nonprecious electrocatalysts: Linking surface science to coordination chemistry. *J. Am. Chem. Soc.* **2013**, *135*, 15443–15449. [CrossRef]
26. Campos-Roldán, C.A.; González-Huerta, R.G.; Alonso-Vante, N. Experimental Protocol for HOR and ORR in Alkaline Electrochemical Measurements. *J. Electrochem. Soc.* **2018**, *165*, J3001–J3007. [CrossRef]